ADVANCED QUANTUM TECHNOLOGIES
www.advquantumtech.com

Critical Energies and Wigner Functions of the Stationary States of the Bose Einstein Condensates in a Double-Well Trap

D. J. Nader and E. Serrano-Ensástiga*

The quartic double-well potential contains the essential ingredients to study many-body systems within a rich semiclassical phase-space that includes an unstable point associated to the critical energy. This critical energy in the quantum realm causes symmetry breaking of the wavefunctions and produces a logarithmic divergence in the density of states, leading to an excited-state quantum phase transition (ESQPT). On the other hand, the Bose–Einstein Condensates (BEC) represent a promising platform to observe quantum mechanical phenomena at a macroscopic level. In this work, the lowest stationary states of the BEC in the mean field approximation are obtained via the Gross–Pitaevskii equation in a double-well trap. The critical energy at which the corresponding wavefunctions experience the symmetry breaking is estimated. It is also found that this critical energy is shifted from the local maximum of the trap as the interaction between bosons increases. The Wigner function is used to obtain a phase space representation of the stationary states. It is observed that the state with closest mean energy to its critical value shows vestiges of the separatrix in the semiclassical phase-space. The trends of the entropy, the nonorthogonality of the stationary states, and the nonclassicality via the negativities of the Wigner function are also examined.

1. Introduction

The double-well potential is one of the favorite confinement traps to explore the peculiar properties of the spectrum and dynamics of a quantum system.[1–3] The symmetry breaking over the center of coordinates caused by the extra barrier in the double-well potential[4–7] produces a transition on the ground state wavefunction from one to two global minima. This phenomenon makes the double well an ideal model to test tunneling effects and quantum-classical correspondence.[8–13] Additionally, the presence of an unstable fixed point in the phase space (generated by the local maximum) is related to the separatrix in the semiclassical phase-space, which separates two different kind of trajectories. In particular, the dynamics of quantum states with probability densities localized near to the separatrix are more susceptible to tunneling transitions and an exponential growth in the out-of-time-ordered correlators.[14–16] All the previous phenomena described above are consequences of a "Excited-state quantum phase transition" (ESQPT).[17] The signature of ESQPTs is a logarithmic divergence in the Density of States at the critical energy that can be observed in the discrete spectrum of the double well.[18] The theoretical predictions of quantum systems confined in double-well potentials have been tested and used in experiments with superconducting circuits,[19] periodically driven quantum systems[20–22] and cold atom systems[23,24] whose effective Hamiltonian is that of the double well.

On the other hand, Bose–Einstein condensates (BEC) offer unprecedented opportunities to study the underlying physics mentioned above due to the astonishing precision and control levels achievable in experiments.[25,26] Of special interest is the promise to extend quantum-mechanical phenomena, particularly wavefunction interference, up to a macroscopic level when a large fraction of bosons occupy the lowest quantum state. One of the main examples of BEC in a double well is the Josephson junction implemented by two linked Bose–Einstein condensates in a double-well potential, where macroscopic tunneling oscillations are observed.[27,28] Analog BECs systems in double-well potentials have been also explored, such as spinor BECs,[29–31] or toroidal BECs, also called atom SQUIDS.[32] On the theoretical side, the spectra, dynamics, and tunneling phenomena of BECs confined in double-well potentials have been also studied,[33–43] including double wells generated by Gaussian functions[44,45] or by a quartic polynomial.[46] Semiclassical approximations[45,47,48]

D. J. Nader
Department of Optics
Faculty of Science
Palacký University
Olomouc 77146, Czech Republic
E-mail: daniel.juliannader@upol.cz

E. Serrano-Ensástiga
Institut de Physique Nucléaire
Atomique et de Spectroscopie
CESAM
University of Liège
Liège B-4000, Belgium

The ORCID identification number(s) for the author(s) of this article can be found under https://doi.org/10.1002/qute.202400451

DOI: 10.1002/qute.202400451

suggest that the rich properties of the phase space of the double well are preserved in the case of the BEC. Since the many-body problem is quite challenging in the general case, simplifications are made such as the use of 1D condensates, which have been realized experimentally,[49,50] and the mean-field approximation that derives the well-known Gross–Pitaevskii (GP) equation.[25,51,52] Another well-known theoretical approach is the finite multimode model, that considers a truncated Hilbert space for the single quantum states of the cold atoms.[25,53,54]

In this work, we employ a self-consistent method to obtain the stationary states of the BEC in a double-well trap. We estimate the critical parameters of the trap at which the lowest stationary states experience the symmetry breaking and their corresponding critical energy. We study the dependency of the critical energy with respect to the atom–atom interaction of the condensate. We use the Wigner function to obtain a phase space representation of the stationary states and examine the behavior of the negativities as the nonlinearity increase. The paper is organized as follows. After the compilation in Section 2 of the theoretical elements needed in this work, we expose the numerical method used in Section 3. We proceed to review the critical values of the parameters of the trap at which symmetry breaking occurs. We first discuss its physical consequences in the limit case of the linear Schrödinger equation in Section 4. We then present the main body of our results associated with the nonlinearity aspects of the GP equation in the mean-field approximation Section 5. Section 6 summarizes our findings and offers some thoughts on future work.

2. Theory

Let us consider a 1D-BEC gas of N atoms, with mass m, and at low energies such that the predominant boson-boson interactions are produced by point-contact collisions.[25] We also adopt the mean-field approximation that assumes the fully condensed wavefunction Φ as the product of normalized single-particle wavefunctions

$$\Phi(\mathbf{r}_1, \ldots, \mathbf{r}_N) = \prod_{i=1}^{N} \Psi(\mathbf{r}_i) \tag{1}$$

with

$$\int |\Psi(\mathbf{r})|^2 \, \mathrm{d}\mathbf{r} = 1 \tag{2}$$

The time-independent GP equation which governs the dynamics of the 1D BEC in the mean-field approximation reads[25,51,52]

$$\left(-\frac{\hbar^2}{2m}\frac{d^2}{dx^2} + V(x) + \beta|\Psi(x,t)|^2 - i\hbar\frac{\partial}{\partial t}\right)\Psi(x,t) = 0 \tag{3}$$

where m is the mass of the identical bosons. The coupling factor β of the nonlinear term in the GP equation is proportional to the s-wave scattering length of the boson-boson interaction a_s, $\beta = 4\pi N\hbar^2 a_s/m$. The stationary solutions for the 1D-BEC can be obtained by solving the time independent GP equation

$$\left(-\frac{\hbar^2}{2m}\frac{d^2}{dx^2} + V(x) + \beta|\Psi_n(x)|^2\right)\Psi_n(x) = \mu_n\Psi_n(x) \tag{4}$$

where $\mu_n = \mu_n'/N$ is the chemical potential μ_n' per particle. In the limit of vanishing nonlinear interactions $\beta \to 0$, there are stationary solutions of Equation (3) which reduce to the eigenfunctions of the associated Schrödinger equation.[55] In this work, we focus in the stationary solutions of the GP equation $\Psi_n(x)$ which tend to the nth-eigenfunction of its respective Schrödinger equation for small β. Correspondingly, these stationary solutions can be sorted according to the energy (8). The trap considered in this work is the quartic or Higgs potential in the form of a symmetric double well (Mexican hat)

$$V(x) = -ax^2 + bx^4 \tag{5}$$

where a is a positive parameter. The parameter b of the double-well potential (5) can be absorbed in the other variables by the Szymanzik rescaling[56]

$$(\tilde{x}, \tilde{a}, \tilde{b}, \tilde{\beta}, \tilde{\mu}) = \left(b^{1/6}x, \frac{a}{b^{2/3}}, 1, \frac{\beta}{b^{1/3}}, \frac{\mu}{b^{1/3}}\right) \tag{6}$$

and

$$\tilde{\Psi}(\tilde{x}) = \Psi(x) \tag{7}$$

Among other double well traps, the quartic double well allows to explore a full family of potentials since it only contains one effective parameter. Furthermore, the local maximum, associated to the critical energy and the separatrix of the phase space, remains fixed at zero. The critical energy and the local maximum of the trap deviate only in the non linear scenario as we will show in the next sections. In the following, we will work with the scaled variables and suppress the tilde symbol in each term. Once the eigenfunctions $\Psi_n(x) = \Psi_n$ are known, the energy of the condensate per particle is given by the expectation value[25,57]

$$E_n = \int \left(\frac{1}{2m}\left|\frac{\mathrm{d}\Psi_n}{\mathrm{d}x}\right|^2 + V(x)|\Psi_n|^2 + \frac{\beta}{2}|\Psi_n|^4\right)\mathrm{d}x \tag{8}$$

In order to obtain a quantum phase-space representation of the BEC stationary states, one can use the Wigner function.[58] It is a function of the position x and momentum p as follows

$$W_n(x,p) = \int \langle x+y|\rho_n|x-y\rangle e^{\frac{2ipy}{\hbar}}\,\mathrm{d}y \tag{9}$$

where $\rho_n = |\Psi_n\rangle\langle\Psi_n|$ is the density matrix of the n−th stationary state. The Wigner function is considered a quasi-probability distribution as it can acquire negative values. However, it successfully describes the marginal distribution $P(x) = \int W(x,p)dp = |\Psi(x)|^2$ after integrating the momentum variable.[59] Thus, the presence of negative regions is not a bug but the central feature of interference of waves in phase space.[60] In experiments of quantum tomography,[61] where the quantum states are reconstructed, it is confirmed that negativities are the main source of non classicalities as they distinguish classical from quantum states. It is worthy to mention that non classical states are promising tools towards the develop of new technologies in quantum computing[62] and information processing.[63]

The volume of the integrated negative part of the Wigner function $W_\rho(x,p)$ is interpreted as a measure of nonclassicality,[64]

$$\delta(\rho) = \int\int |W_\rho(x,p)|\,\mathrm{d}x\,\mathrm{d}p - 1 \tag{10}$$

Recent studies suggest that negative Wigner functions are necessary for witnessing tunneling.[65] In any case, the Wigner function of the stationary states has the vestiges of the classical trajectories.[9] In particular, the negativities of the wavefunction of the BEC offer an special opportunity to witness nonclassical phenomena at a macroscopic level. On the other hand, the entropy of the states is only properly defined in terms of the Wigner function only if it is positive anywhere.[66]

The phase-space representation of the states of the BEC provided by the Wigner function[60] is complementary to the one given by the Husimi function.[67] The Husimi function is defined in terms of a coherent state $|\alpha\rangle$ as

$$Q_n(x,p) = \frac{1}{\pi}\langle\alpha|\rho_n|\alpha\rangle \tag{11}$$

whose complex parameter α defines the average position and momentum $\alpha = \frac{1}{\sqrt{2}}(\bar{x} + i\bar{p})$. Though the Husimi function fails to satisfy the marginal distribution,[59] it allows to quantify the entropy of the states since it is positive everywhere. Thus, we can use the Wehrl entropy[68]

$$S_n = \int Q_n(x,p)\log Q_n(x,p)\,dx\,dp \tag{12}$$

to quantify the information or uncertainty encoded in the stationary states of the BEC.

Lastly, following the WKB approximation for BEC condensates with small β,[69,70] the transmission coefficient from one well to the other reads

$$T_n = \exp\left(-\frac{2}{\hbar}\gamma_n\right)$$
$$\gamma_n = \int_{x_1}^{x_2}\sqrt{2m\big(V(x)+\beta|\Psi_n(x)|^2-\mu_n\big)}\,\mathrm{d}x \tag{13}$$

where $x_{1,2}$ are the classical turning points in the effective potential of the GP equation (3). Throughout the rest of the paper, we consider $m = \hbar = 1$.

3. The Numerical Method

In this work, we employ the method of Finite-Difference discretization of the Schrödinger equation[71] and a self-consistent algorithm to incorporate the nonlinear term.[72] In the Finite-Difference method, the configuration space $x \in [-L, L]$ is divided in D subintervals of length $\Delta = 2L/D$ such that $x_\alpha = -L + \alpha\Delta$, where $\alpha = 0, 1, .., D$. We take a sufficiently large D such that the first derivative of the wavefunction $\frac{\mathrm{d}\Psi_n}{\mathrm{d}x}$ at each x_α is well approximated by

$$\frac{\mathrm{d}\Psi_n(x_\alpha)}{\mathrm{d}x} \approx \frac{\Psi_n(x_{\alpha+1}) - \Psi_n(x_\alpha)}{\Delta} \tag{14}$$

Repeating this argument, the formula to calculate the second derivative appearing in the kinetic energy, is given by

$$\frac{\mathrm{d}^2\Psi_n(x_\alpha)}{\mathrm{d}x^2} \approx \frac{\Psi_n(x_{\alpha+1}) - 2\Psi(x_\alpha) + \Psi_n(x_{\alpha-1})}{\Delta^2} \tag{15}$$

By using the approximation above, the GP equation (3) takes the form of an eigenvalue problem

$$A_n^{(k)}\Psi_n^{(k)} = \mu_n^{(k)}\Psi_n^{(k)} \tag{16}$$

where $A_n^{(k)} = -\frac{\hbar^2}{2m}A_1 + A_2 + \beta A_{3,n}^{(k)}$ is a $(D+1)\times(D+1)$ matrix composed by the tridiagonal matrix

$$A_1 = \begin{pmatrix} -2 & 1 & & & \\ 1 & -2 & 1 & & \\ & \ddots & \ddots & \ddots & \\ & & 1 & -2 & 1 \\ & & & 1 & -2 \end{pmatrix} \tag{17}$$

corresponding to the kinetic energy, the diagonal matrices associated to the potential trap and the boson-boson interactions, respectively, with entries

$$\big(A_2\big)_{rs} = V(x_{r-1})\delta_{rs}\,, \quad \Big(A_{3,n}^{(k)}\Big)_{rs} = |\Psi_n^{(k-1)}(x_{r-1})|^2\delta_{rs} \tag{18}$$

The superindex (k) indicates the corresponding iteration step of each element. In particular, the matrix $A_{3,n}^{(k)}$ is built with the nth-eigenfunction of the previous iteration, with initial wavefunction assumed as a normalized constant function $\Psi_n^{(0)}(x_\alpha) = \sqrt{N/2L}$. The Equation (16) is solved via selfconsistent field (SCF) until reaching convergence of both the eigenvalues and eigenfunctions up to the orders

$$\left|\mu_n^{(k)} - \mu_n^{(k-1)}\right| < 10^{-9}\,, \quad 1 - |\langle\Psi^{(k)}|\Psi^{(k-1)}\rangle| < 10^{-4} \tag{19}$$

The value of L is considered such that the solution fulfills $|\Psi(\pm L)| \approx 10^{-3}$ and, consequently, its probability density outside the interval $[-L, L]$ is negligible. It is known that the simplest SCF method converges towards a solution of the nonlinear Equation (3) or oscillates between two independent states which are not solutions.[73] An analog difficulty can be found in the Iterative Hartree—Fock Procedure that involves recalculation of the one-electron density matrix.[74,75] In some cases the level shifting algorithm circumvents this convergence problem.[73] It is also known that, if the nonlinearity parameter β is small, the SCF method is able to reach convergence.[75,76] The number of iterations required to match the convergence criteria (18) depends on the parameters a and β. However, within the domain of weak interaction $\beta \leq 2$, we observe that a maximum of 30 iterations are needed to reach convergence with our numerical method and starting from our initial guess. Once the wavefunction of the stationary state is obtained, any integral can be calculated approximately by

$$\int f(x)\,\mathrm{d}x \approx \Delta\sum_{\alpha=1}^{D} f(x_\alpha) \tag{20}$$

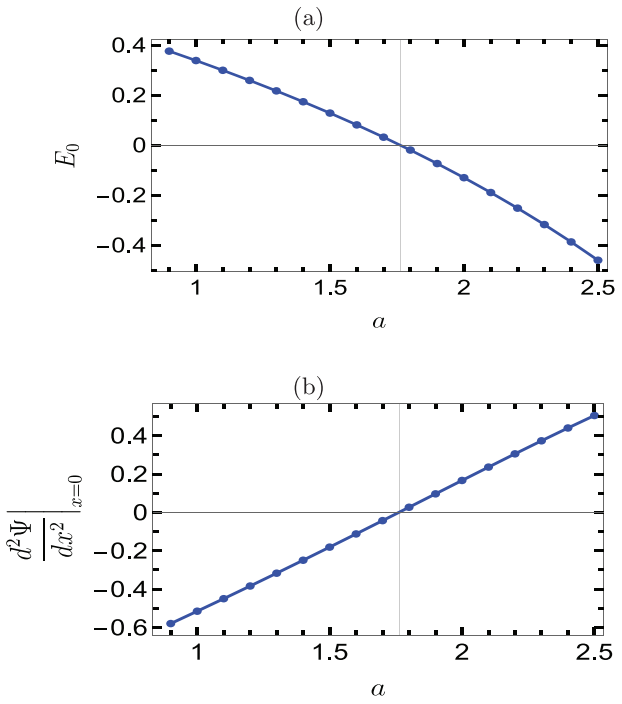

Figure 1. Energy (a) and second derivative of the ground state evaluated at the center of coordinates (b) as a function of the parameter a. The parameter β is set to zero to coincide with the Schrödinger equation with the quartic double-well potential. The vertical gray line indicates the transition at the critical parameter, both at $a_c = 1.7616$, associated with the change of sign of the respective quantity.

In particular, Equation (20) can be used to obtain the energy (8) of the stationary state. Considering a grid along the position and momentum variables, we can also apply Equation (20) to obtain efficiently the Wigner function of the stationary states (9) while the resolution can be easily tuned by increasing the number of subintervals D.

The dynamics of an initial state $|\psi_0\rangle$ over a time period T, can be well approximated by introducing an additional discretization of time[72] $\Delta' = T/D'$ where D' are the number of small steps of time. From there we can apply the time-evolution operator to estimate the wave function at any time step $U(t_i)|\psi(t_{i-1})\rangle$. The time evolution operator is given by

$$U(t_i) = \exp\left(\frac{-i\Delta'}{\hbar}\left(-\frac{\hbar^2}{2m}A_1 + A_2 + \beta A_4^{(i-1)}\right)\right) \tag{21}$$

where $\left(A_4^{(i-1)}\right)_{rs} = |\psi(x_{r-1}, t_{i-1})|^2 \delta_{rs}$.

4. The Schrödinger Limit of the GP Equation

We start the analysis from the limit case of the Schrodinger equation $\beta = 0$ in order to shed some light on the properties of the stationary states of the GP equation when the nonlinear term is weak.

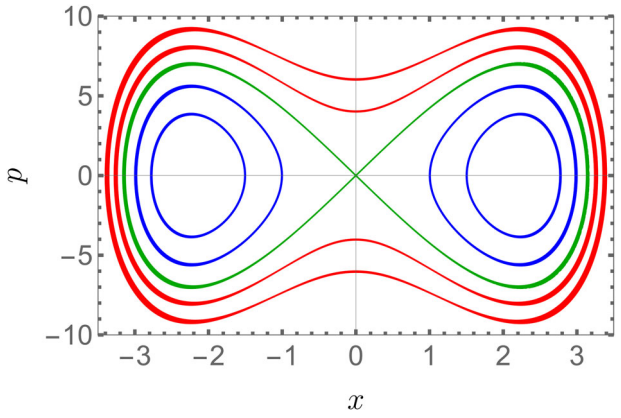

Figure 2. Classical trajectories of the double well in the linear case ($\beta = 0$). The black line indicates the separatrix at the critical energy $E_c = 0$, and the blue (red) lines are trajectories with energies below (above) the critical. The effective parameter of the potential is $a = 10$.

4.1. Symmetry Breaking and Critical Parameters

The local maximum of the double well (6) at $x = 0$ represents a critical energy $E_c = 0$ for the Schrödinger equation ($\beta = 0$)[18] since the distribution of energy levels is different above or below this value. It is well known that the energy of the ground state might be either positive or negative[77] depending on the value of the effective parameter of the trap a. As the parameter a increases, there is a particular value for which the energy of the ground state passes from positive to negative, i.e., the energy becomes less than the local maximum. This transition is known as symmetry breaking. For the case of quartic double potential, this symmetry breaking have been explored recently.[78] In a nutshell, the phenomena can be described as follows: if the wells are close to each other (bound case), the wavefunction has a concave shape at the center of the trap with a global maximum at $x = 0$. On the contrary, if the wells are too separated to each other, the wavefunction changes to be convex around $x = 0$ once we cross the phase transition. The shape of the new wavefunction has now one minimum at $x = 0$ between two maxima. Intermediate cases are challenging to determine. However, the second derivative of the wavefunction evaluated at the midpoint of the double well is sensitive to this transition. The phase transition of the wavefunction is a natural consequence of symmetry breaking in degenerated wells which can be observed theoretically and experimentally with molecules where the nuclei play the roll of the wells (see Ref. [79] for an example).

The critical parameter a_c can be estimated either by analysing the sign of the ground state energy or the sign of the second derivative of the ground-state wavefunction (15) evaluated at the midpoint $x = 0$. By the numerical calculations plotted in **Figure 1** of both quantities as functions of a, we conclude that both criteria match and the effective critical parameter of the trap is $a_c \approx 1.7616$. The critical parameters of the general trap $(\tilde{a}, \tilde{b})$ can be recovered by using the Szymanzik rescaling (6). Needless to mention that each stationary state is associated to a critical parameter where the symmetry breaking of the wavefunction occurs, however the critical energy remains fixed for any state at the local maximum of the trap

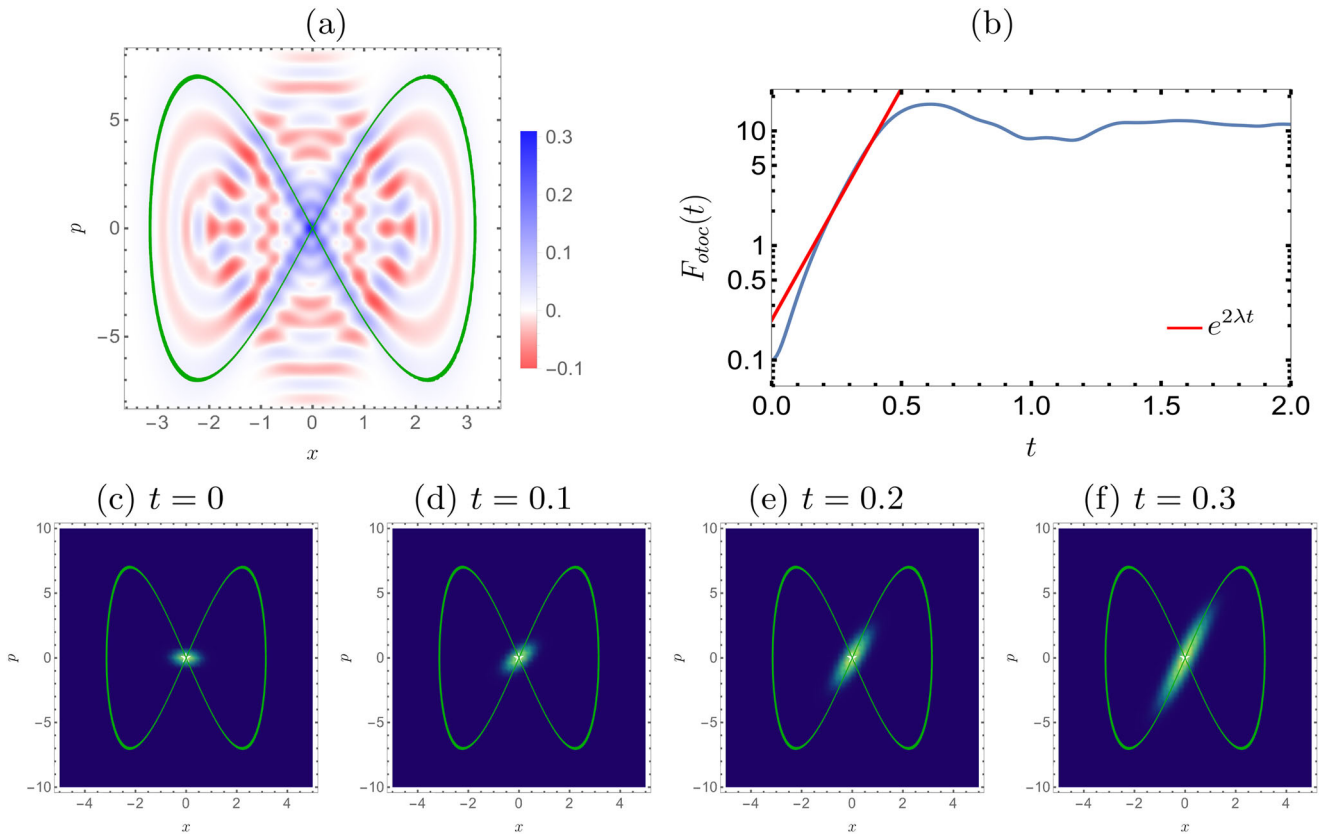

Figure 3. a) Density of the Wigner function of the stationary state ($n = 10$) with closest energy to the critical $E_c = 0$. b) Fidelity Out-Of-Order Correlator (Fotoc) in Logarithmic scaled of an initial coherent state $|\alpha(x_0, p_0)\rangle$ lying along the separatrix. The slope of the exponential growth can be compared against the positive Lyapunov exponent $\lambda = \sqrt{2a}$ of the fixed point $(x_0, p_0) = 0, 0$. c–f). Time evolution of an initial coherent state initially centered at the center of the phase space. The green line correspond to the separatrix of the classical phase space All cases correspond to the linear limit $\beta = 0$ and the parameter of the trap $a = 10.83$ is chosen such that the energy of the nth-state with $n = 10$ matches with the critical energy $E_c = 0$.

($E_c = 0$), i.e., there is only one critical energy in the Schrödinger limit.

4.2. Phase Space and Wigner Function

The classical trajectories of the double well are shown in **Figure 2**. We can observe the presence of a separatrix, associated to the critical energy ($E_c = 0$), which includes the center of the phase space. The center of the phase space, in turns, is an unstable fixed point with positive Lyapunov exponent,[18] and it is accompanied by some interesting implications on the quantum dynamics.[15]

The Wigner function of the stationary state with closest energy to the critical $E_c = 0$ shows the vestiges of the separatrix, as depicted in **Figure 3**(a). The time evolution of an initial coherent state illustrate the relevance of the unstable point in the phase space and the critical energy. It can be obtained by using the evolution operator (21), or alternatively, use an open source like.[80] Also in Figure 3 bottom panels, it can be observed that the coherent state centered at the unstable point $(x, p) = (0, 0)$ spreads along the separatrix. Interestingly, coherent quantum states with initial conditions close to the separatrix show an exponential growth of the Fidelity Out-of-time order Correlator (FOTOC) $\mathcal{F}_{otoc}(t) = \sigma_x(t) + \sigma_p(t)$ which is equal to the addition of the variance of position x and momentum p. We can observe in Figure 2(b) that its slope matches with the positive Lyapunov exponent associated to the unstable fixed point. This is an indication that the initial coherent states close to the separatrix (or equivalently has mean energy close to the critical $E \approx 0$) experience fast delocalization. This phenomenon, among others, are associated to ESQPTs. They have been recently reported also for BEC in spin systems.[81–83]

5. The Bose Einstein Condensate

5.1. Shifting the Critical Energy

We now consider the GP equation of a condensate gas (3) with finite atom-atom interaction $\beta > 0$. Here, the critical parameter a_c can only be estimated by using the criterion of the second derivative because the *effective* potential of the atoms contains the additional positive interaction $\beta|\Psi|^2$, and hence the critical energy E_c may be different than its value in the Schrödinger scenario $E_c = 0$. In **Figure 4**, we show how the critical parameter of the ground states is shifted for different values of β. One can associate a critical energy in the GP scenario by evaluating Equation (8) at the critical parameter a_c and its respective wavefunction. We found that both critical parameters and critical energy

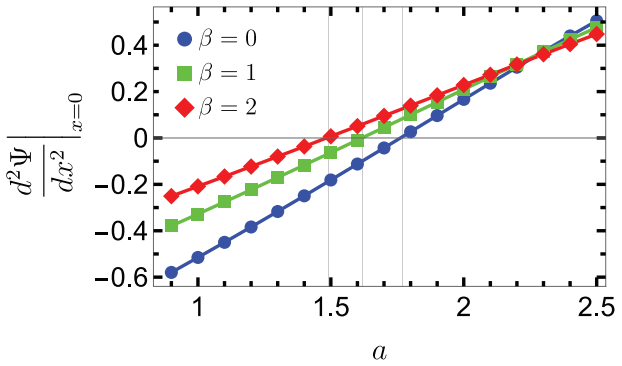

Figure 4. Second derivative of the ground-state wave function evaluated at the origin as a function of the parameter a for different values of β.

Table 1. Critical parameter of the trap and critical energy of the stationary states of the BEC.

n	Critical parameter	Critical energy
0	$a_c(\beta) = 1.7616 - 0.1513\beta + 0.0061\beta^2$	$E_c(\beta) = 0.2662\beta - 0.0034\beta^2$
2	$a_c(\beta) = 4.3567 - 0.1156\beta + 0.0023\beta^2$	$E_c(\beta) = 0.2865\beta - 0.0026\beta^2$
4	$a_c(\beta) = 6.2886 - 0.1012\beta + 0.0017\beta^2$	$E_c(\beta) = 0.3001\beta - 0.0019\beta^2$
6	$a_c(\beta) = 7.9539 - 0.0950\beta + 0.0027\beta^2$	$E_c(\beta) = 0.3123\beta - 0.0023\beta^2$
8	$a_c(\beta) = 9.4550 - 0.0857\beta + 0.0014\beta^2$	$E_c(\beta) = 0.3192\beta - 0.0014\beta^2$
10	$a_c(\beta) = 10.8430 - 0.0808\beta + 0.0016\beta^2$	$E_c(\beta) = 0.3282\beta - 0.0024\beta^2$

fit to quadratic functions of the nonlinear parameter β. The criterion of the second derivative to estimate the critical parameter and critical energies can be repeated for any stationary state with positive parity. We present the fits for the critical parameters and the critical energies in **Table 1**. We can confirm that, contrary to the Schrödinger limit, each state is associated to a different critical energy and they are in general deviated from the local maximum of the potential. The shift of the critical energy has some implications on the information content in the stationary states. As illustrated in **Figure 5**, the Wehrl entropy contained in the stationary states of the BEC is minimum when the energy of the state matches $E_c/2$.

5.2. The Wigner Function

Figure 6 shows the Wigner function (9) of the ground state ($n = 0$) of the BEC in the double-well for different traps (controlled by the parameter a) and strength of the nonlinear term (controled by the parameter β). One can appreciate that the negative regions of the Wigner function lies along the momentum axis and the center of the phase space is a global maximum originated by the interference pattern. Closer to the critical parameter of the trap a_c (see top row of Figure 6 for $a = 2$), the Wigner function contains only one peak with shoulders centered at the local minima of the trap which eventually becomes in separated peaks if the double well is deep enough (bottom row for $a = 5$). Negative regions are more pronounced in the latter case. The Wigner function of stationary states plays the role of the classical trajectories in quantum mechanics.[9] Semiclassical approximations for the BEC[47,48,84] suggest that the trajectories in the GP case have the same properties that those of the linear case. However, the critical energy associated to the separatrix is shifted from the local maximum of the trap, as discussed in the previous subsection. To verify this point, we adjust the parameter of the trap such that the energy of the stationary state $n = 4$ matches with the shifted critical energy of the BEC $E_c(\beta = 2) = 0.546$. We plot $W_4(x, p)$ in **Figure 7**.

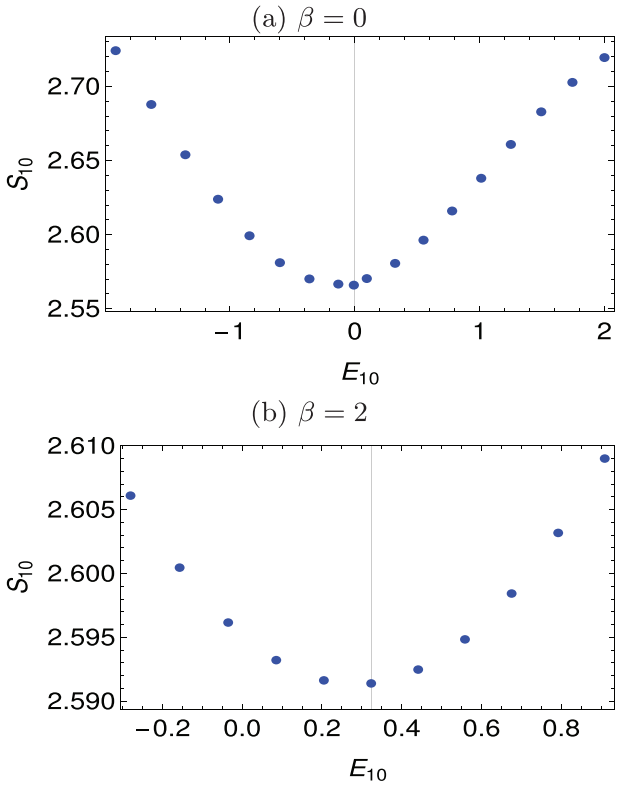

Figure 5. Wehrl entropy of the stationary state $n = 10$ as a function of the mean energy. The figures are obtained by scanning the effective parameter of the trap a in the vicinity of the critical value. The vertical lines indicate $E_c/2$.

5.3. Nonclassicalities

The resolution reached with the finite difference method allows to quantify the negativities of the Wigner function even if the effective parameter of the trap a is small. We can now explore the dependence of the nonclassicality of the ground state $\delta(\rho_0)$ (10) with respect to β (see **Figure 8**) for $a = 2$ and $a = 5$. It is worth to mention that, even in the absence of boson-boson interactions ($\beta = 0$), the nonlinear forces of the double-well potential produce negative regions of the Wigner function.[85] We observe in Figure 8 that the volume of the integrated negative part of the Wigner function changes as a function of the parameter β, i.e., the nonclassical behavior of the BEC is affected with the interaction between bosons. However, the monotonous deviation of $\delta(\rho_0)$ with respect to β depends on the parameter of the trap a. To scrutinize the possible connection of the negativities and the tunneling we calculate the transmission coefficient using the WKB approximation (13) and the energy gap between the ground and the first excited states $\Delta E = E_1 - E_0$.

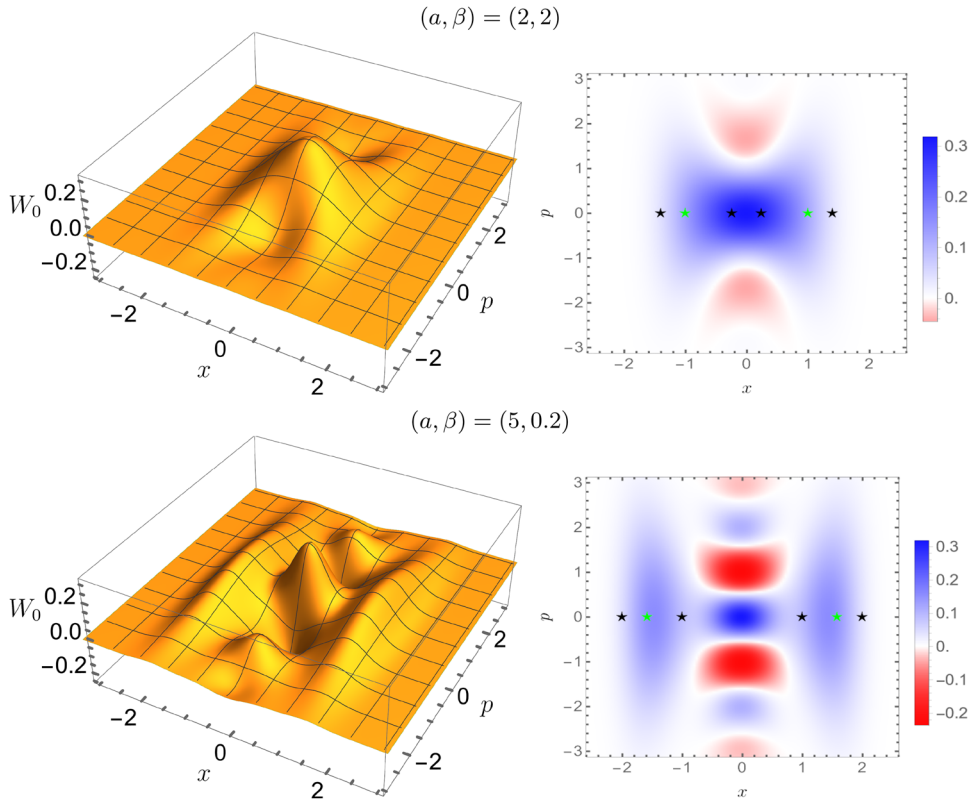

Figure 6. Wigner functions (left column) of the ground state of the BEC in a double-well trap and its density (right column) for the case different combinations of the parameters $(a, \beta) = (2, 2)$ and (5,0.2), respectively. The black stars represent the classical turning points, and the green ones the bottom of the degenerated wells.

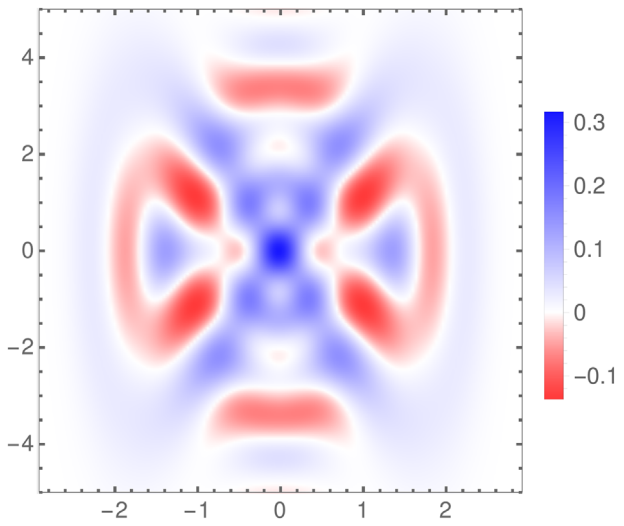

Figure 7. $W_4(x, p)$ with the trap parameter such that the mean energy matches with the critical energy.

It is known that in the Schrödinger scenario, the transmission coefficient is proportional with respect to the energy gap.[86] We plot in Figure 8 ΔE in the BEC case, as a function of β for the values of $a = 2$ and $a = 5$. For the case of smaller effective parameter $a \approx 2$, ΔE increases roughly linearly with respect to β while the coefficient of transmission decrease. One can comprehend this by considering the enlargement of the effective barrier width encountered by the stationary state, thereby impeding its ability to penetrate the energy barrier. On the other hand, for $a \approx 5$, while ΔE increases again roughly linearly, the transmission coefficient increase with respect to β as well. A potential explanation is that the width of the effective potential is barely modified at the bottom of the well, and then its penetration is enhanced with β. Contrary to the Schrödinger scenario ($\beta = 0$), the energy gap and the transmission coefficient are not proportional quantities.

For $a = 5$, the double well is deep enough to contain four stationary solutions of the GP Equation (4), whose mean energies (8) are below the critical in Table 1. The energy (8) levels, are presented schematically in **Figure 9**. It is observed that the first pair of energy states are quasidegenerated and close to the bottom of the double well. The energy gap increases for the second pair of energy levels since they are closer to the local maximum. A similar behavior was observed in the case of Gaussian wells.[44]

5.4. Nonorthogonality of the Stationary States

Nonlinear quantum mechanics, such as the GP equation, might have nonorthogonal stationary states.[87] This can be understood by the fact that the extra nonlinear terms in the corresponding nonlinear Schrödinger equation act as an extra effective potential. In the case of the GP equation (3), the effective potential

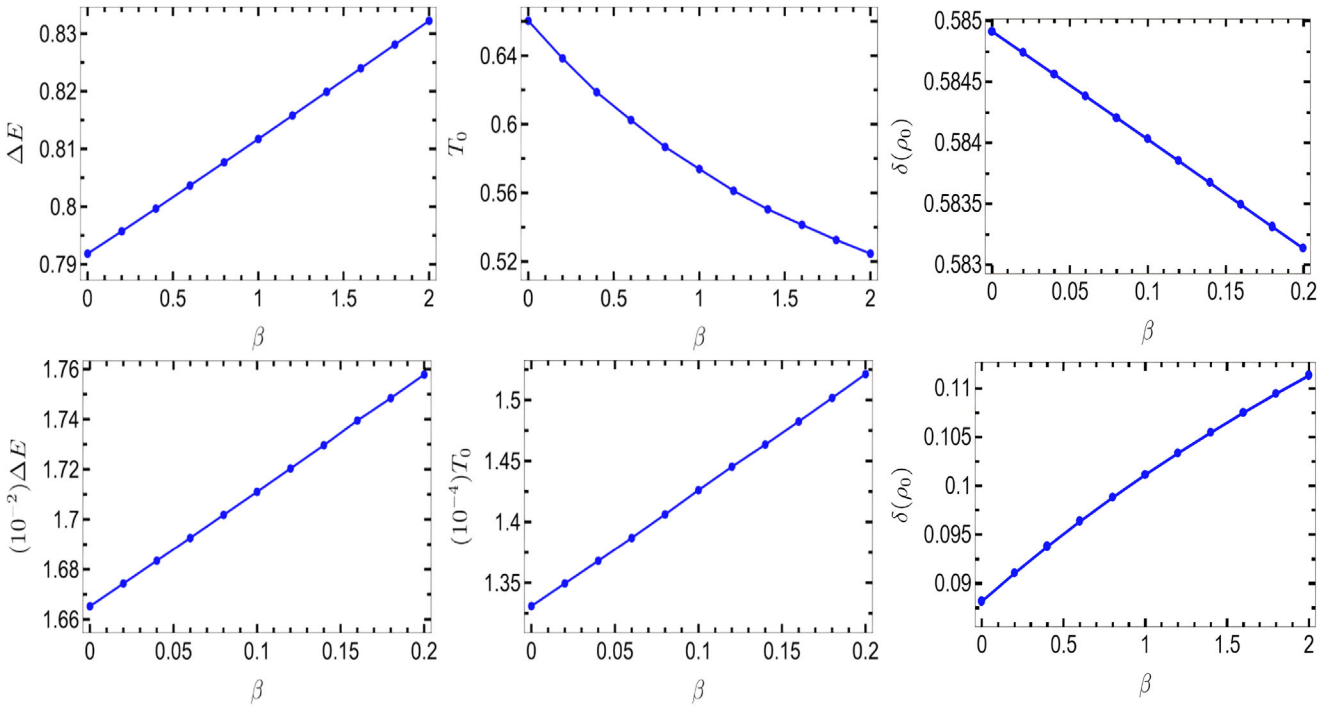

Figure 8. Volume of the negative part of the Wigner function $\delta(\Psi_0)$, energy splitting ΔE of the ground and first excited states, and transmission coefficient T_0 as a function of the parameter β. The rows correspond to $a = 2$ (top) and 5 (bottom), respectively.

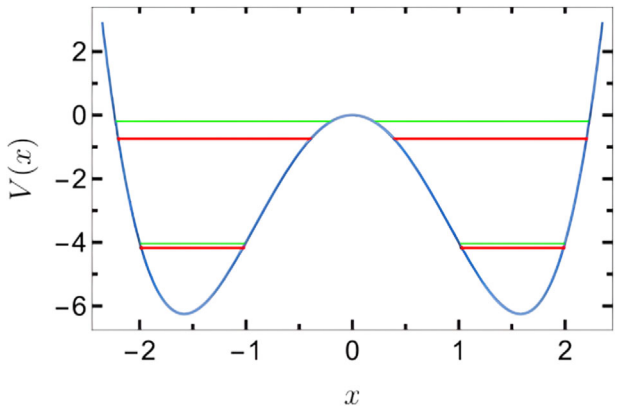

Figure 9. R2.3. Double well quartic trap $a = 5$ (solid blue line) and the four lowest mean energies (8) of the BEC for $\beta = 0.1$. For the mean energies (8) we use the solutions of the non linear GP Equation (4) as wave functions. The states with even(odd) parity are denoted in red (green).

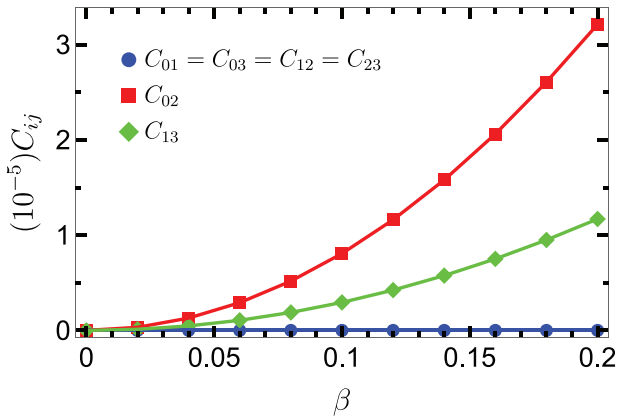

Figure 10. β-dependency of the overlaps among the stationary functions with the lowest energies $C_{ij} = |\langle\Psi_i|\Psi_j\rangle|^2$ where $i = 1, 2, 3, 4$. The parameter of the double well is fixed at $a = 5$.

includes $\beta|\Psi|^2$. Consequently, the eigenstates come from different effective potentials. We plot in **Figure 10** the overlap between the first stationary states $C_{ij} = |\langle\Psi_i|\Psi_j\rangle|^2$ for $a = 5$ as a function of β. We observe the unchanged orthogonality of states with different parity. On the contrary, states with the same parity become less orthogonal as β increases. The nonorthogonality of the states is a signature of a nonlinear unitary evolution, which are useful in algorithms to distinguish nonorthogonal states, in order to solve the unstructured search problem,[88] and to devise nonunitary quantum gates such as feasible nonlinear Hadamard gates.[89]

6. Conclusions and Perspectives

We carried out an extensive analysis of the stationary states of the 1D BECs confined in a double-well potential and obtained their representation in the quantum phase space through the Wigner function. The stationary states experiences a symmetry breaking which is quite sensitive to the sign of the second derivative of the wavefunction at the midpoint of the double well. This criterion was exploited to estimate the critical parameters of the trap and the associated critical energies of the lowest stationary states. We confirm that the critical energy matches with the local maximum of the potential only in the limit case of vanishing non linearity.

However, in the BEC the critical energy of the stationary states is deviated from the local maximum of the double well by the presence of the non linearity of the GP. We have obtained the trend of the effective critical parameters a_c of the quartic double-well trap with respect to the strength of the interparticle interaction β and the corresponding critical energies of the lowest states. The critical energy and the symmetry breaking in the wavefunction observed in the BEC are indications of the presence of an ESQPT. However, this yet has to be confirmed with a non-analytical behavior of the density of states.

We have also observed that the Wigner function of the stationary state with closest energy to the critical has vestiges of the separatrix of the semiclassical phase space. Negativities are generated inside the separatrix because of the interference. Furthermore, the entropy content in the stationary states is a local minimum if the mean energy is half of the critical energy. This result contributes to state engineering in Bose-Einstein condensates leveraging the interference generated by state superposition, i.e., the Wigner negativities and their trends, as well as the information encoded in stationary states.

Additionally, we scrutinize the tendency, as β increases, of the nonclassicality, the energy gap between consecutive energy levels, the tunneling transmission coefficient through the energy barrier, and the nonorthogonality of the stationary states. Contrary to the Schrödinger scenario, the energy gap and the transmission coefficient are not proportional quantities in the BEC case. On the other hand, the nonclassicality and the transmission coefficient follow the same tendency as β increases.

The analysis and methodology presented in this work can be replicated using alternative double-well trap configurations. In particular, the results motivate future investigations into Gaussian double wells, which are commonly used to model energy barriers in experiments with ultracold atoms. If the wells are close to each other, the results can be reproduced by adjusting the quartic double-well configuration. However, significant discrepancies might arise as the separation between the wells increases.

Even though our article concentrates in the static aspects of the GP equation, the Wigner function of stationary states shed some light on the dynamics as they are the analogous in quantum mechanics to the classical trajectories. Moreover, the Wigner formalism is equally applicable to the dynamics in the phase space of non stationary states of the BEC by using the density matrix of the evolved state $\rho(t) = |\psi(t)\rangle\langle\psi(t)|$. The exponential growth of the fotoc and the possible tunneling motivates a further study of the dynamics of the Wigner function of the BEC.

Acknowledgements

The authors thank R . Filip for his valuable comments. E.S.E. acknowledges support from the postdoctoral fellowship of the IPD-STEMA program of the University of Liège (Belgium). D.J.N. acknowledges the support from grant CZ.02.01.01/00/22_008/0004649 (QUEENTEC) provided by the EU and MEYS of the Czech Republic.

Open access publishing facilitated by Univerzita Palackeho v Olomouci, as part of the Wiley - CzechELib agreement.

Conflict of Interest

The authors declare no conflict of interest.

Data Availability Statement

All codes, scripts, supplemental formulas, and data needed to reproduce the results in this manuscript are available online https://github.com/djuliannader/GrossPitaevskiiSCF.

Keywords

Bose–Einstein condensates, double-well potential, Gross–Pitaevskii, Wigner functions

Received: September 13, 2024
Revised: December 30, 2024
Published online:

[1] E. V. Vybornyi, *Theor. Math. Phys.* **2014**, *178*, 93.
[2] M. A. P. Reynoso, D. J. Nader, J. Chávez-Carlos, B. E. Ordaz-Mendoza, R. G. Cortiñas, V. S. Batista, S. Lerma-Hernández, F. Pérez-Bernal, L. F. Santos, *Phys. Rev. A* **2023**, *108*, 033709.
[3] G. Theocharis, P. G. Kevrekidis, D. J. Frantzeskakis, P. Schmelcher, *Phys. Rev. E* **2006**, *74*, 056608.
[4] J. Joger, A. Negretti, R. Gerritsma, *Phys. Rev. A* **2014**, *89*, 063621.
[5] E. Delabaere, F. Pham, *Ann. Phys* **1997**, *261*, 180.
[6] T. Meier, S. Petitgirard, S. Khandarkhaeva, L. Dubrovinsky, *Nat. Commun.* **2018**, *9*, 1.
[7] Q. Dong, G.-H. Sun, M. A. Aoki, C.-Y. Chen, S.-H. Dong, *Mod. Phys. Lett. A* **2019**, *34*, 1950208.
[8] J. Plata, J. M. G. Llorente, *J. Phys. A Math. Theor.* **1992**, *25*, L303.
[9] M. Novaes, *J. opt., B Quantum semiclass.* **2003**, *5*, S342.
[10] S. Murmann, A. Bergschneider, V. M. Klinkhamer, G. Zürn, T. Lompe, S. Jochim, *Phys. Rev. Lett.* **2015**, *114*, 080402.
[11] U. Weiss, H. Grabert, P. Hänggi, P. Riseborough, *Phys. Rev. B* **1987**, *35*, 9535.
[12] G. Rastelli, *Phys. Rev. A* **2012**, *86*, 012106.
[13] G. Lu, W. Hai, H. Zhong, *Phys. Rev. A* **2009**, *80*, 013411.
[14] H. Hasegawa, *Physica A* **2013**, *392*, 6232.
[15] J. R. Cary, P. Rusu, *Phys. Rev. A* **1993**, *47*, 2496.
[16] J. Chávez-Carlos, T. L. Lezama, R. G. Cortiñas, J. Venkatraman, M. H. Devoret, V. S. Batista, F. Pérez-Bernal, L. F. Santos, *npj Quantum Inf.* **2023**, *9*, 76.
[17] P. Cejnar, P. Stránskỳ, M. Macek, M. Kloc, *J. Phys. A: Math. Theor.* **2021**, *54*, 133001.
[18] D. Nader, J. Hernández-González, H. Vázquez-Sánchez, S. Lerma-Hernández, *Phys. Lett. A* **2023**, *481*, 129014.
[19] R. Harris, M. W. Johnson, S. Han, A. J. Berkley, J. Johansson, P. Bunyk, E. Ladizinsky, S. Govorkov, M. C. Thom, S. Uchaikin, B. Bumble, A. Fung, A. Kaul, A. Kleinsasser, M. H. S. Amin, D. V. Averin, *Phys. Rev. Lett.* **2008**, *101*, 117003.
[20] J. Venkatraman, R. G. Cortinas, N. E. Frattini, X. Xiao, M. H. Devoret, A driven quantum superconducting circuit with multiple tunable degeneracies, **2023**.
[21] E. Kierig, U. Schnorrberger, A. Schietinger, J. Tomkovic, M. K. Oberthaler, *Phys. Rev. Lett.* **2008**, *100*, 190405.
[22] M. Marthaler, M. I. Dykman, *Phys. Rev. A* **2007**, *76*, 010102.
[23] I. Lesanovsky, T. Schumm, S. Hofferberth, L. M. Andersson, P. Krüger, J. Schmiedmayer, *Phys. Rev. A* **2006**, *73*, 033619.
[24] S. Hofferberth, I. Lesanovsky, B. Fischer, J. Verdu, J. Schmiedmayer, *Nat. Phys.* **2006**, *2*, 710.
[25] C. J. Pethick, H. Smith, *Bose-Einstein condensation in dilute gases*, Cambridge University Press, Cambridge **2008**.

[26] M. Lewenstein, A. Sanpera, V. Ahufinger, *Ultracold Atoms in Optical Lattices: Simulating quantum many-body systems*, Oxford University Press, Oxford **2012**.
[27] M. Albiez, R. Gati, J. Fölling, S. Hunsmann, M. Cristiani, M. K. Oberthaler, *Phys. Rev. Lett.* **2005**, *95*, 010402.
[28] T. Schumm, S. Hofferberth, L. M. Andersson, S. Wildermuth, S. Groth, I. Bar-Joseph, J. Schmiedmayer, P. Krüger, *Nat. Phys.* **2005**, *1*, 57.
[29] D. M. Stamper-Kurn, H.-J. Miesner, A. P. Chikkatur, S. Inouye, J. Stenger, W. Ketterle, *Phys. Rev. Lett.* **1999**, *83*, 661.
[30] A. T. Black, E. Gomez, L. D. Turner, S. Jung, P. D. Lett, *Phys. Rev. Lett.* **2007**, *99*, 070403.
[31] Y. Eto, H. Shibayama, H. Saito, T. Hirano, *Phys. Rev. A* **2018**, *97*, 021602.
[32] C. Ryu, P. W. Blackburn, A. A. Blinova, M. G. Boshier, *Phys. Rev. Lett.* **2013**, *111*, 205301.
[33] B. Juliá-Díaz, J. Martorell, A. Polls, *Phys. Rev. A* **2010**, *81*, 063625.
[34] B. Juliá-Díaz, J. Martorell, M. Melé-Messeguer, A. Polls, *Phys. Rev. A* **2010**, *82*, 063626.
[35] A. U. J. Lode, A. I. Streltsov, O. E. Alon, H.-D. Meyer, L. S. Cederbaum, *J. Phys. B: At., Mol. Opt. Phys.* **2009**, *42*, 044018.
[36] V. Kenkre, in *Interplay of Quantum Mechanics and Nonlinearity: Understanding Small-System Dynamics of the Discrete Nonlinear Schrödinger Equation*, Springer, Berlin **2022**, pp. 231–257.
[37] J. D. Andersen, S. Raghavan, V. Kenkre, *Int. J. Mod. Phys. B* **2022**, *36*, 2240003.
[38] A. C. Pflanzer, S. Zöllner, P. Schmelcher, *Phys. Rev. A* **2010**, *81*, 023612.
[39] B.-L. Hu, H. Dong, Y. Ma, *J. Phys. B: At., Mol. Opt. Phys.* **2019**, *52*, 195302.
[40] V. S. Shchesnovich, M. Trippenbach, *Phys. Rev. A* **2008**, *78*, 023611.
[41] H. C. Prates, D. A. Zezyulin, V. V. Konotop, *Phys. Rev. Res.* **2022**, *4*, 033219.
[42] F. Bello, P. R. Eastham, *Phys. Rev. B* **2017**, *95*, 245312.
[43] T. Paul, K. Richter, P. Schlagheck, *Phys. Rev. Lett.* **2005**, *94*, 020404.
[44] S. Zöllner, H.-D. Meyer, P. Schmelcher, *Phys. Rev. A* **2008**, *78*, 013621.
[45] E. W. Kirr, P. G. Kevrekidis, E. Shlizerman, M. I. Weinstein, *SIAM J. Math. Anal.* **2008**, *40*, 566.
[46] M. Jääskeläinen, P. Meystre, *Phys. Rev. A* **2005**, *71*, 043603.
[47] D. Pelinovsky, T. Phan, *J. Diff. Eqns.* **2012**, *253*, 2796.
[48] J. L. Marzuola, M. I. Weinstein, *arXiv preprint arXiv:0912.1706* **2009**.
[49] T. Kinoshita, T. Wenger, D. S. Weiss, *Science* **2004**, *305*, 1125.
[50] J. Esteve, J.-B. Trebbia, T. Schumm, A. Aspect, C. I. Westbrook, I. Bouchoule, *Phys. Rev. Lett.* **2006**, *96*, 130403.
[51] E. P. Gross, *Nuovo Cimento (1955-1965)* **1961**, *20*, 454.
[52] L. P. Pitaesvkii, *Sov. Phys. JETP* **1961**, *13*, 451.
[53] E. A. Ostrovskaya, Y. S. Kivshar, M. Lisak, B. Hall, F. Cattani, D. Anderson, *Phys. Rev. A* **2000**, *61*, 031601.
[54] D. Ananikian, T. Bergeman, *Phys. Rev. A* **2006**, *73*, 013604.
[55] R. D'Agosta, B. A. Malomed, C. Presilla, *Phys. Lett. A* **2000**, *275*, 424.
[56] A. V. Turbiner, *Int. J. Mod. Phys. A* **2010**, *25*, 02n647.
[57] C. M. Dion, E. Cancès, *Comput. Phys. Commun.* **2007**, *177*, 787.
[58] J. Weinbub, D. K. Ferry, *Appl. Phys. Rev.* **2018**, *5*, 041104.
[59] E. Colomés, Z. Zhan, X. Oriols, *J. Comput. Electron.* **2015**, *14*, 894.
[60] J. Teske, M. R. Besbes, B. Okhrimenko, R. Walser, *Phys. Scr.* **2018**, *93*, 124004.
[61] G. M. D'Ariano, M. G. Paris, M. F. Sacchi, *Adv. Imaging Electron Phys.* **2003**, *128*, S1076.
[62] A. Grimm, N. E. Frattini, S. Puri, S. O. Mundhada, S. Touzard, M. Mirrahimi, S. M. Girvin, S. Shankar, M. H. Devoret, *Nature* **2020**, *584*, 205.
[63] L. Li, C.-L. Zou, V. V. Albert, S. Muralidharan, S. M. Girvin, L. Jiang, *Phys. Rev. Lett.* **2017**, *119*, 030502.
[64] A. Kenfack, K. Życzkowski, *J. opt., B Quantum semiclass. opt.* **2004**, *6*, 396.
[65] Y. L. Lin, O. C. O. Dahlsten, *Phys. Rev. A* **2020**, *102*, 062210.
[66] Z. Van Herstraeten, N. J. Cerf, *Phys. Rev. A* **2021**, *104*, 042211.
[67] K. W. Mahmud, H. Perry, W. P. Reinhardt, *Phys. Rev. A* **2005**, *71*, 023615.
[68] S. Floerchinger, T. Haas, H. Müller-Groeling, *Phys. Rev. A* **2021**, *103*, 062222.
[69] D. R. Lindberg, N. Gaaloul, L. Kaplan, J. R. Williams, D. Schlippert, P. Boegel, E.-M. Rasel, D. I. Bondar, *J. Phys. B* **2023**, *56*, 025302.
[70] J. X. de Carvalho, M. S. Hussein, W. Li, *Phys. Rev. A* **2008**, *78*, 032906.
[71] A. M. Halpern, Y. Ge, E. D. Glendening, *J. Chem. Educ.* **2022**, *99*, 3053.
[72] V. A. Trofimov, N. V. Peskov, *Math. Model. Anal.* **2009**, *14*, 109.
[73] E. Cancès, *SCF algorithms for HF electronic calculations*, Springer Berlin Heidelberg, Berlin, Heidelberg **2000**, pp. 17–43, ISBN 978-3-642-57237-1.
[74] J. Kouteckỳ, V. Bonačić, *J. Chem. Phys.* **1971**, *55*, 2408.
[75] C. Yang, W. Gao, J. C. Meza, *SIAM J. Matrix Anal. Appl.* **2009**, *30*, 1773.
[76] E. Cancès, G. Kemlin, A. Levitt, *SIAM J. Matrix Anal. Appl.* **2021**, *42*, 243.
[77] D. Gonzalez, J. Chávez-Carlos, J. G. Hirsch, J. D. Vergara, *Phys. Scr.* **2024**.
[78] H. C. Rosu, S. C. Mancas, P. Chen, *Ann. Phys.* **2014**, *349*, 33.
[79] H. Xu, Z. Li, F. He, X. Wang, A. Atia-Tul-Noor, D. Kielpinski, R. Sang, I. Litvinyuk, *Nat. Commun.* **2017**, *8*, 15849.
[80] S. Krämer, D. Plankensteiner, L. Ostermann, H. Ritsch, *Comput. Phys. Commun.* **2018**, *227*, 109.
[81] Z.-X. Niu, Q. Wang, *Phys. Rev. A* **2023**, *107*, 033307.
[82] Z.-X. Niu, Q. Wang, *Phys. Rev. E* **2024**, *110*, 064112.
[83] R. Zheng, J. Qin, B. Chen, Z. Yu, L. Zhou, *Opt. Express* **2024**, *32*, 25207.
[84] R. H. Goodman, J. L. Marzuola, M. I. Weinstein, Self-trapping and josephson tunneling solutions to the nonlinear schrödinger / gross-pitaevskii equation, **2015**, https://www.aimsciences.org/article/id/73403340-9021-463f-80b5-00e858b8b5ff.
[85] R. Hudson, *Rep. Math. Phys.* **1974**, *6*, 249.
[86] L. D. Landau, E. M. Lifshitz, *Quantum mechanics: non-relativistic theory*, vol. *3*, Elsevier, Amsterdam **2013**.
[87] C. Schwartz, *J. Math. Phys.* **1997**, *38*, 484.
[88] A. M. Childs, J. Young, *Phys. Rev. A* **2016**, *93*, 022314.
[89] S. Xu, J. Schmiedmayer, B. C. Sanders, *Phys. Rev. Res.* **2022**, *4*, 023071.